




Article

# A Simple Technique for Studying Chaos Using Jerk Equation with Discrete Time Sine Map

Muhammad Haseeb Arshad <sup>1</sup>, Mahmoud Kassas <sup>1</sup>, Alaa E. Hussein <sup>1,\*</sup> and Mohammad A. Abido <sup>1,2</sup>

<sup>1</sup> Department of Electrical Engineering, King Fahd University of Petroleum & Minerals, Dhahran 31261, Saudi Arabia; haseeb.arshad.ee@gmail.com (M.H.A.); mkassas@kfupm.edu.sa (M.K.); mabido@kfupm.edu.sa (M.A.A.)

<sup>2</sup> K. A. CARE Energy Research & Innovation Center, Dhahran 31261, Saudi Arabia

\* Correspondence: husseina@kfupm.edu.sa; Tel.: +966-13-8604868

**Abstract:** Over the past decade, chaotic systems have found their immense application in different fields, which has led to various generalized, novel, and modified chaotic systems. In this paper, the general jerk equation is combined with a scaled sine map, which has been approximated in terms of a polynomial using Taylor series expansion for exhibiting chaotic behavior. The paper is based on numerical simulation and experimental verification of the system with four control parameters. The proposed system's chaotic behavior is verified by calculating different chaotic invariants using MATLAB, such as bifurcation diagram, 2-D attractor, Fourier spectra, correlation dimension, and Maximum Lyapunov Exponent. Experimental verification of the system was carried out using Op-Amps with analog multipliers.

**Keywords:** chaos; jerk equation; sine map; bifurcation; Lyapunov exponent; Poincare section; correlation dimension



**Citation:** Arshad, M.H.; Kassas, M.; Hussein, A.E.; Abido, M.A. A Simple Technique for Studying Chaos Using Jerk Equation with Discrete Time Sine Map. *Appl. Sci.* **2021**, *11*, 437. <https://doi.org/10.3390/app11010437>

Received: 18 October 2020  
Accepted: 24 December 2020  
Published: 4 January 2021

**Publisher's Note:** MDPI stays neutral with regard to jurisdictional claims in published maps and institutional affiliations.



**Copyright:** © 2021 by the authors. Licensee MDPI, Basel, Switzerland. This article is an open access article distributed under the terms and conditions of the Creative Commons Attribution (CC BY) license (<https://creativecommons.org/licenses/by/4.0/>).

## 1. Introduction

Chaos theory focuses on the fact that a complex system's solutions are not really because of the noise or the irregularities that appear, instead because of the interaction of the system components. Chaos can be loosely defined as a fascinating intermediate state between randomness and steady behavior, and it has been a subject of growing research over the last decade [1]. Chaotic systems are characterized by their sensitive dependency on the initial conditions, which leads to deterministic aperiodic bounded behavior impossible to predict in the long term [2]. These characteristics find their application in various practical systems such as biology, chemistry, secure communications [3], bits generators, cryptography [4], mechanical engineering [5,6], machine drives [7], and ecology. Being able to mathematically describe a system that negates the scientific viewpoint about the practical systems and can depict chaos is an accomplishment of science [8].

A continuous chaotic system defined in terms of differential equations usually surpasses the discrete chaotic system defined in terms of difference equations because of the added complexity and chaotic dynamics. Because of the growing demands of finding a more generalized chaotic system, researchers are comparing the merits and demerits of these systems. Few attempts are made to combine both these classes of system ideas and develop a better solution in terms of easy implementation using simple Op-Amps [9].

The qualitative nature of the solutions of a dynamical system described by a simple ordinary differential equation (ODE) depends on the dynamical system's degree. As the degree increases, the solutions start to arrange themselves on a strange attractor in phase space [10]. The minimum degree required to get a strange attractor is three, as studied in [11]. Although a simple jerk equation with one nonlinear function provides an appropriate framework for visualizing chaotic behavior, the necessary conditions for the onset of chaos in an autonomous dynamical system of ODEs are still unknown [12].

Despite the fact that non-autonomous and autonomous systems have become increasingly straightforward over the last three decades, they have remained predominant models for studying different bifurcation diagrams and aperiodic deterministic behavior in nonlinear dynamics [12,13]. Many simple nonlinear electronic circuits capable of showing this erratic behavior have been proposed in the literature [14–17]. These systems can be described in terms of ordinary differential (or difference) equations; examples of such systems are the Colpitts oscillator [18,19], Chua’s circuit [20,21], Jerk circuit [22,23], and many more. These circuits use one or more nonlinear elements with an active component for exhibiting chaos while allowing one or more control parameters to control this behavior’s intensity.

The most prominent of the autonomous chaotic systems is Chua’s circuit and Jerk circuit. Initially, the most popular way of generating chaos was to enforce a nonlinear function in the system capable of creating different equilibrium points by varying one of the non-linearity parameters introduced in the system. This method resulted in many practically unrealistic dynamical systems. To ensure the realistic analog/digital implementation of the chaotic circuit, Randwan et al. proposed a chaotic circuit where a digitally controlled MOS-transistor acted as a source of non-linearity and was capable of generating multi-scroll attractors [24]. In 2011, Bao et al. replaced the nonlinear part of Colpitts oscillator with a more practical triangular function and validated their proposed circuit numerically and experimentally [25]. In [26], the use of staircase nonlinear term for chaos generation was studied by Zidan et al. C. Sanchez et al. proposed a saturated nonlinear function series (SNFSs) and modified the generic Chua’s circuit to form a chaotic circuit for producing chaotic oscillations at high frequency [27,28]. The experimental validation for SNFSs was carried out in [29] by Ortega et al. later on. Sprott studied different variants of the jerk equation using simple nonlinear terms [11,30] that could be easily practically realizable compared to the nonlinear component of the Chua’s circuit [31,32]. The jerk equation has the third derivative of ‘ $x$ ’ (position), where the 1st derivative is the velocity, the 2nd derivative is the acceleration, and the 3rd derivative is the Jerk. A detailed analysis for the family of jerky equations to exhibit chaotic behavior was done in [33].

In the last decade, many researchers have proposed their chaotic circuit based on a jerk equation. The simplest of all was reported in [22], which utilized a single Op-Amp circuit with a FET operating in the triode mode as a source of non-linearity. Other notable contributions were from J. Kengne et al., who used hyperbolic and exponential nonlinear terms with the jerk equation [34,35]. Recently R. Tange et al. introduced a more generalized exponential non-linearity  $\phi k(x) = 0.5(\exp(kx) - \exp(-x))$ , which reduces to hyperbolic sine function for  $k = 1$ , with jerk equation for producing chaos.

Although in most of the literature reported, authors have used nonlinear function with the jerk equation. Still, only a single effort has been reported where a discrete chaotic map is used with the jerk equation as a nonlinear function [9]. In this paper, a discrete sine map is added as a nonlinear function in the jerk equation to get the single scroll chaotic attractor. The proposed system is vibrant in terms of chaotic behavior and can be easily implemented using any generic Op-Amp with very little hassle.

The rest of the paper is organized as follows: Section 2 outlines the problem description; Section 3 briefly discusses the proposed methodology. In Section 4, eigenvalue analysis for the proposed chaotic system is carried out; Section 5 summarizes the detailed numerical simulations for the proposed system, Experimental validation is mentioned in Section 6, discussion and conclusion are summed up in Sections 7 and 8.

## 2. Problem Description

The jerk equation has been an extensive research topic for the last four decades for the scientific community. The general form of this equation is

$$\ddot{x} + \alpha\dot{x} + \beta x + f(x) = 0 \quad (1)$$

where,  $f(x)$  corresponds to added non-linearity. This third-order differential equation can be transformed into a system of three first-order differential equations by simple substitution [36].

$$\dot{x}_1 = x_2 \quad (2)$$

$$\dot{x}_2 = x_3 \quad (3)$$

$$\dot{x}_3 = -\alpha x_3 - \beta x_2 - f(x) \quad (4)$$

It is to be noted that the added non-linearity can be a function of any state  $(x_1, x_2, x_3)$ . In this paper, the nonlinear term added is the function of the first state i.e.,  $f(x) = f(x_1)$ . The choice of  $f(x_1)$  can lead to a new jerk based chaotic system. Here, the discrete sine map is integrated with the above jerk equation to get a novel jerk based chaotic system.

### 3. Proposed Methodology

The simple sine map given in Equation (5) has been a part of literature for quite some time [37].

$$x_{n+1} = R \times [\sin \pi x_n] \quad (5)$$

here, 'R' is called the control parameter

Using the Taylor series expansion, it can be approximated as follows

$$x_{n+1} = R \times \left[ \pi x_n - \frac{(\pi x_n)^3}{6} + H.O.T \right] \quad (6)$$

By ignoring the higher-order terms (H.O.T.), the approximated sine map can be easily realized using Op-Amps which produces comparable results. The effect of the control parameter (R) variations for this approximated discrete sine map is further characterized by finding the bifurcation diagram, maximum Lyapunov exponent, cobweb plot and time series plot as shown in Figure 1.

This approximated map is added as a nonlinear function of the state  $x_1$  i.e.,  $f(x_1)$  in the Equation (4) to get the modified jerk based chaotic system

$$\dot{x}_1 = x_2 \quad (7)$$

$$\dot{x}_2 = x_3 \quad (8)$$

$$\dot{x}_3 = -\alpha x_3 - \beta x_2 - R \times \left[ \pi x_1 - \frac{(\pi x_1)^3}{6} \right] \quad (9)$$

Defining  $R\pi = \sigma$  and  $R(\pi)^3 = \gamma$ , Equation (9) becomes

$$\dot{x}_3 = -\alpha x_3 - \beta x_2 - \sigma x_1 + \frac{\gamma x_1^3}{6} \quad (10)$$

The control parameters ( $\alpha, \beta, \sigma$ , and  $\gamma$ ) can be varied to get different strange attractors. The proposed discrete-time map based jerk system is the simplified autonomous chaotic system capable of depicting different periodic and chaotic attractors.

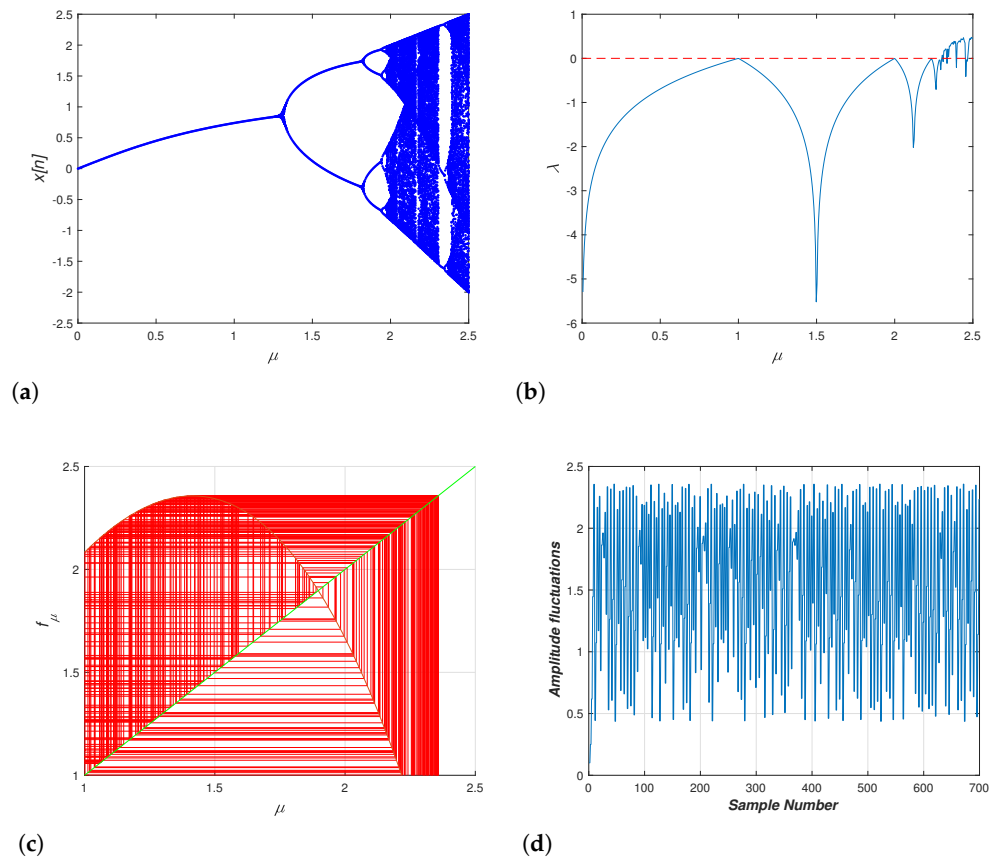


**Figure 1.** Chaotic invariants for approximated discrete-time Sine Map: (a) Bifurcation Diagram, (b) Lyapunov Exponent, (c) Cobweb Plot, (d) Pseudo Space Trajectory, (e) Time Series.

#### 4. Eigenvalue Analysis

The eigenvalue analysis of the proposed jerk chaotic system is carried out to find the stability of the equilibrium points of the system and also to establish the route to chaos with the change in control parameters. To find the eigenvalues, first the Jacobin of the system is calculated given as

$$J = \begin{bmatrix} 0 & 1 & 0 \\ 0 & 0 & 1 \\ 0.5\gamma x^2 - \sigma & -\beta & -\alpha \end{bmatrix} \tag{11}$$

Finally, the eigenvalues are calculated by solving the associated characteristic equation of the system i.e.,

$$\det|J - \lambda I| = 0 \tag{12}$$

$$\Rightarrow \lambda^3 + \alpha\lambda^2 + \beta\lambda - 0.5\gamma x^2 + \sigma = 0 \tag{13}$$

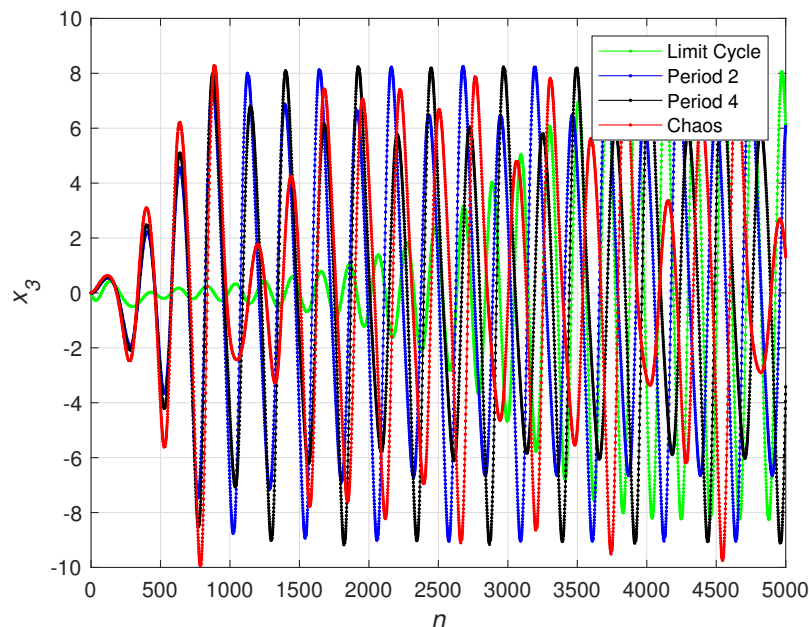
It can be concluded from the Equation (13) that  $E_0(0,0,0)$  is always unstable, whereas the stability of points of the form  $E_{1,2}(\pm 1,0,0)$ ,  $E_{1,2}(0,\pm 1,0)$ ,  $E_{1,2}(0,0,\pm 1)$  depends on the four parameters of the system, i.e.,  $(\alpha, \beta, \gamma, \text{ and } \sigma)$ . In this paper, the control parameters  $(\alpha, \gamma, \text{ and } \sigma)$  are kept constant while  $\beta$  is varied to establish the bifurcation route to chaos of the proposed jerk based chaotic system.

#### 5. Numerical Simulation & Results

Extracting nonlinear measures from time-series is a multifaceted problem, and care must be taken to elucidate its outcomes. Various theoretical measures like Lyapunov

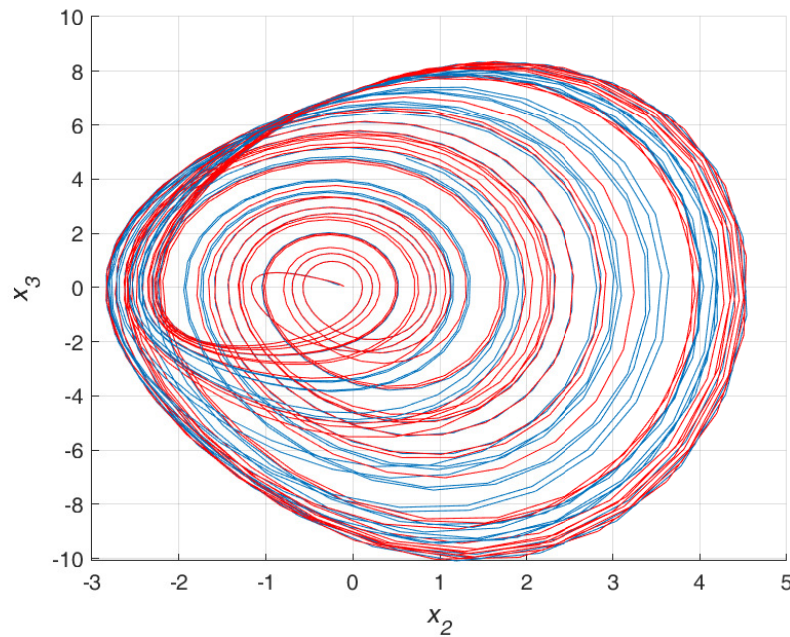
exponent and fractal dimension are used to quantify the chaotic time-series as they are invariants of the attractor. These quantifiers turn a time-series into a single number, which is handy for highlighting important information about the system complexity and degree of freedom (DOF). Chaotic invariants are usually found to validate the presence of chaos, and ensure that the results obtained show sensitive dependence on the initial condition and are not just random white noise. To validate the route to chaos in the proposed system, numerical simulations were carried out in MATLAB. Runge-Kutta method was used to solve the system of Equations (7), (8) and (10). A step-size of  $\Delta t = 0.08$  was used. The values of fixed control parameters  $\alpha$ ,  $\gamma$ , and  $\sigma$  are set to 1, -6, and -6 respectively, throughout the simulations.

Figure 2 shows the resulting time series for  $x_3$  with its values on the y-axis and no. of samples on the x-axis for different values of  $\beta$ . The light green line is for ' $\beta = 9$ ' which shows a period 1 behavior (limit cycle), the blue line is for ' $\beta = 6$ ' which corresponds to period 2 behavior; the black line is for ' $\beta = 5.82$ ' corresponding to period 4, and the red line for ' $\beta = 5.535$ ' shows more interesting aperiodic time series also known as chaotic time series.



**Figure 2.** Time Series for for  $x_3$ : Presence of multiple attractors in the proposed discrete-time map based chaotic jerk system.

The presented system shows the infamous sensitive dependence on the initial conditions of the system. Figure 3 shows the phase portrait between  $x_2$  &  $x_3$  for two different sets of initial conditions for  $(x_1, x_2, \text{ and } x_3)$ .



**Figure 3.** Sensitivity dependence on the initial conditions: Two sets of initial conditions (0.1, 0.1, 0.5) & (0.5, 0.5, 0) with  $\beta = 5.535$ .

#### 5.1. Lyapunov Exponent Test

Lyapunov Exponent test is commonly used for checking the existence of chaos in dynamical systems. If for any dynamical system, one of the Lyapunov exponents is positive, it indicates chaos. There are various algorithms available to find the Maximum Lyapunov Exponent (MLE) spectrum of a system described by differential (or difference) equations [38,39]. The basic equation for finding the Lyapunov exponents is given below [40].

$$\lambda(x_i) = \lim_{n \rightarrow \infty} \frac{1}{n} \sum_{i=0}^{n-1} \ln \left( \left| f'(x_i) \right| \right) \quad (14)$$

where,  $x_i$  is the time series for the  $i$ th ODE.

The dynamic Lyapunov spectrum of the proposed system, calculated using Wolf's algorithm, for the control variable ' $\beta = 5.535$ ' (chaotic case) is shown in Figure 4.

From Figure 4, it can be concluded that one of the Lyapunov spectra is positive. Since the positive Lyapunov exponent implies chaos, the system trajectory will diverge only in one direction, thereby confirming the single scroll attractor shown in Figure 3.

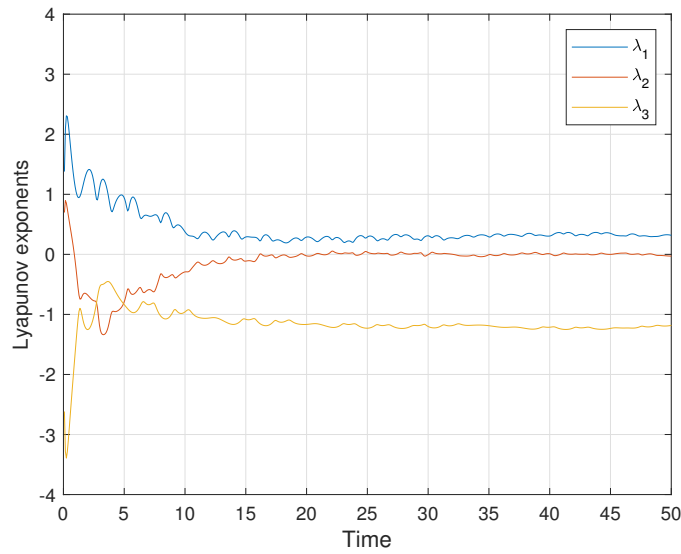


**Figure 4.** Maximum Lyapunov Exponent spectrum for the proposed discrete-time map based chaotic jerk system.

5.2. Bifurcation Diagram

The bifurcation diagram of the proposed system was found by varying control parameter ‘ $\beta$ ’ from 5 to 12 with a step size of 0.01. The initial conditions were set to  $\mathbf{x}_0 = [0.5 \ 0.5 \ 0]'$ , and the period-doubling route to chaos was plotted in Figure 5 for all three states of the system.

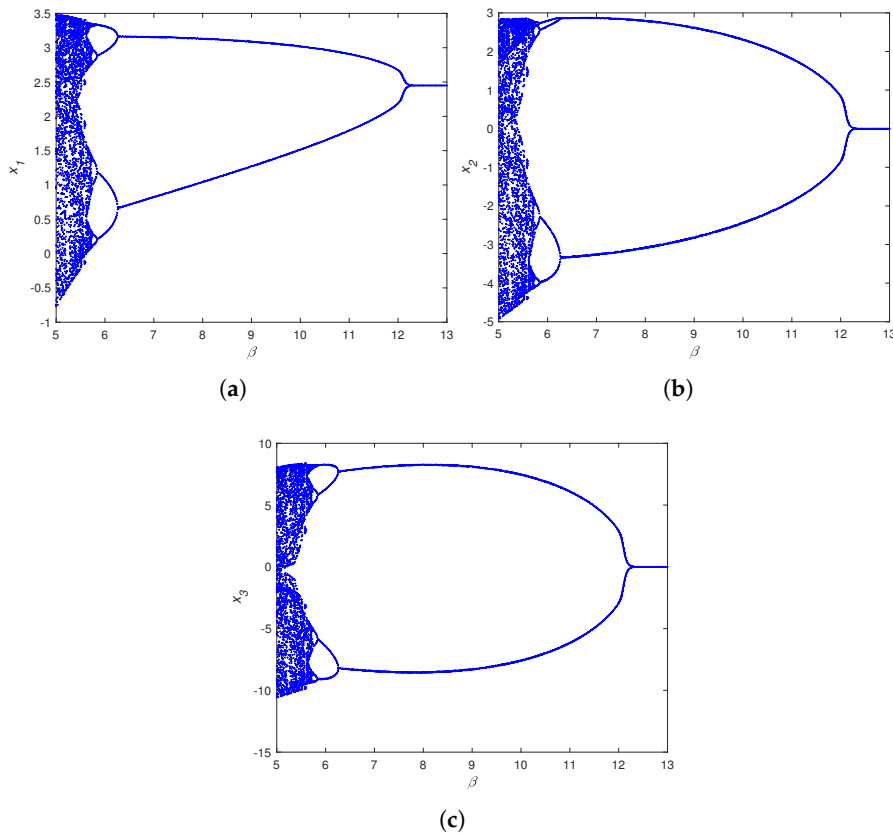


**Figure 5.** Bifurcation Diagram: (a) local maxima of  $x_1$  vs. Control Parameter  $\beta$ , (b) local maxima of  $x_2$  vs. Control Parameter  $\beta$ , (c) local maxima of  $x_3$  vs. Control Parameter  $\beta$ .

It is to be noted that for  $\beta = 18$ , the system has no oscillation, and this value is termed as the critical value. As  $\beta$  starts to decrease from 12 onward, the jerk based system starts to bifurcate from stable period 1 to period-doubling route to chaos shown in Figure 5.

### 5.3. Correlation Dimension

Every chaotic attractor has a fractal structure [41] and exhibits self-similarity (scale-invariance) quantified by computing fractal dimensions. Fractal dimension is a non-integer value that gives insights about the geometric form of the attractor. Correlation dimension provides a good estimate of the fractal dimension of the chaotic attractor. The correlation dimension can be found as

$$D_{cor} = \frac{\log(C_r)}{\log(r)} \quad (15)$$

where,  $C_r$  is called the correlation sum and is defined as

$$C_r = \frac{2}{N(N-1)} \sum_{i=1}^N \sum_{j=i+1}^N \Theta(r - (x_i - x_j)) \quad (16)$$

here, ' $\Theta$ ' is the heavy-side step function, ' $r$ ' is the radius, and  $N$  is the sample length. Figure 6 shows the graph between  $\log(C_r)$  vs.  $\log(r)$ , the slope of which gives the correlation dimension approximately equal to 1.87.

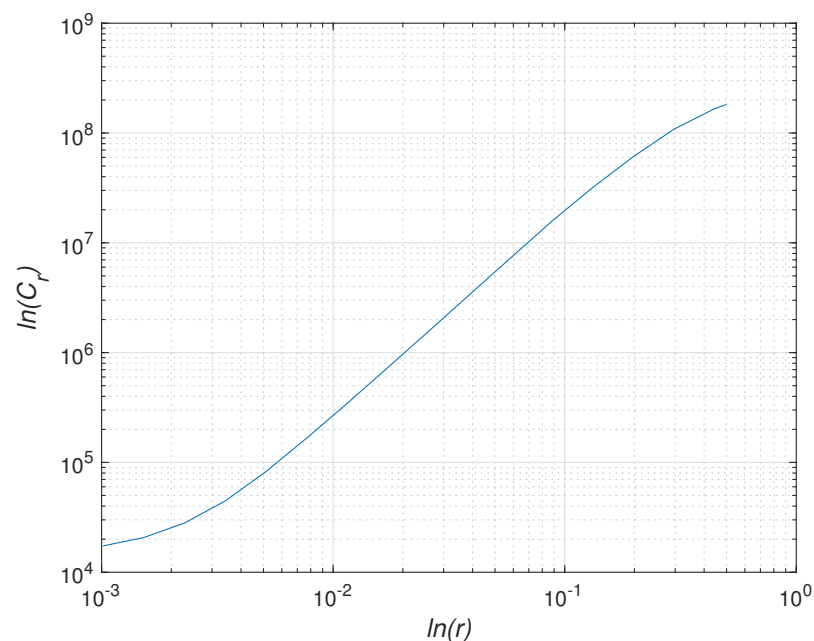


**Figure 6.**  $C_r$  vs.  $\ln(r)$  plot for calculating the Correlation Dimension.

### 5.4. Frequency Spectra

Frequency spectra is an essential visual tool to study chaos in a system. Many researchers have also used wavelet transform instead of frequency spectra as it can not only show the change in the system dynamics but also can point out the time at which such a change has occurred [42]. However, the size of the window plays a pivotal role in getting better visualization in the wavelet transform method. Frequency spectra method was preferred in this paper as it broadly illustrates the frequency dispersion distribution present in the system dynamics, which is enough for the visualization of chaos. Because of the highly chaotic region (5–5.5) in the bifurcation diagram Figure 5, the Fourier power spectrum was calculated only for four different cases. With every variation in the control parameter  $\beta$ , the presence of different attractors with the corresponding Fourier power spectrum is shown in Figure 7.



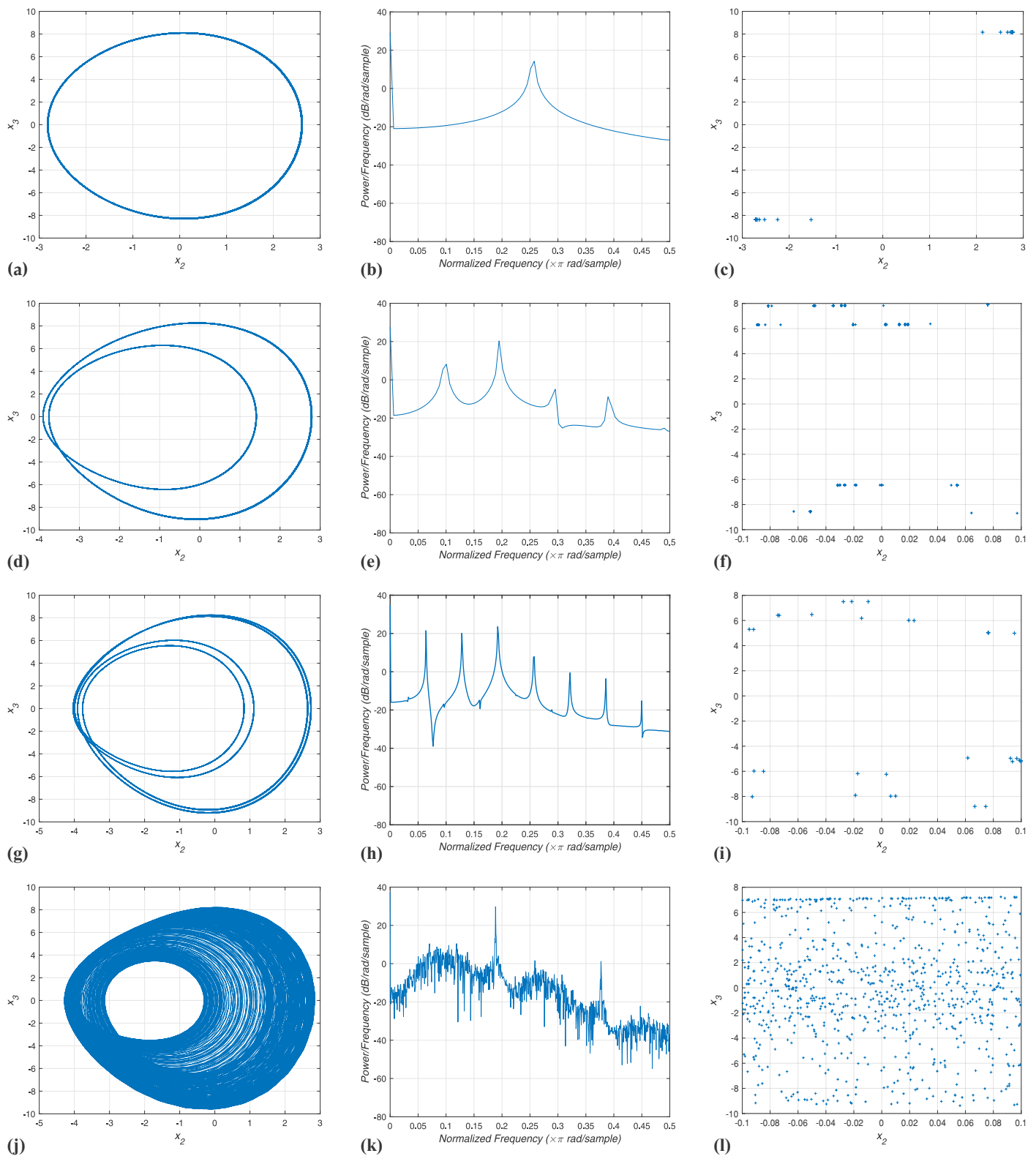


**Figure 7.** Attractor (**left**), Frequency Spectrum (**center**), & Poincare Section: (**right**) (a–c) Period 1 or Limit Cycle Attractor case for  $\beta = 9$ , (d–f) Period 2 Attractor case for  $\beta = 6$ , (g–i) Period 4 Attractor case for  $\beta = 5.84$ , (j–l) Chaotic Attractor case for  $\beta = 5.535$ .

Clearly, one can see by visual inspection that there are 1, 2, and 4 periodic peaks in Figure 7b,e,h respectively corresponding to period 1, period 2 and period 4 attractors

shown in Figure 7a,d,g. Also, an aperiodic power spectrum related to the chaotic attractor shown in Figure 7j is given in Figure 7k.

### 5.5. Poincare Section for Different Attractors

In certain cases, a periodic orbit can be confidently identified from a two-dimensional projection of an attractor (phase portraits). Nevertheless, this process typically does not help in yielding a convincing inference between quasi-periodic and strange attractors. The Poincare section, a two-dimensional plane intersecting the steady-state trajectories as seen in Figure 8, offers a better understanding of the periodicity. It transforms a continuous flow into a discrete mapping of time (Poincare map). Usually, only one direction of the crossing of the trajectory is considered. It is also possible to classify the behavior of the system by analyzing the stroboscopic distribution of the distinct points in the Poincare section. A finite number of points on the Poincare section which adequately represent the periodicity of the motion are observed for a periodic motion. For a quasi-periodic motion, a continuous line in the Poincare map is observed. If the motion is chaotic, because of the fractal character of the chaotic attractors, many irregularly points will be seen on the plane.

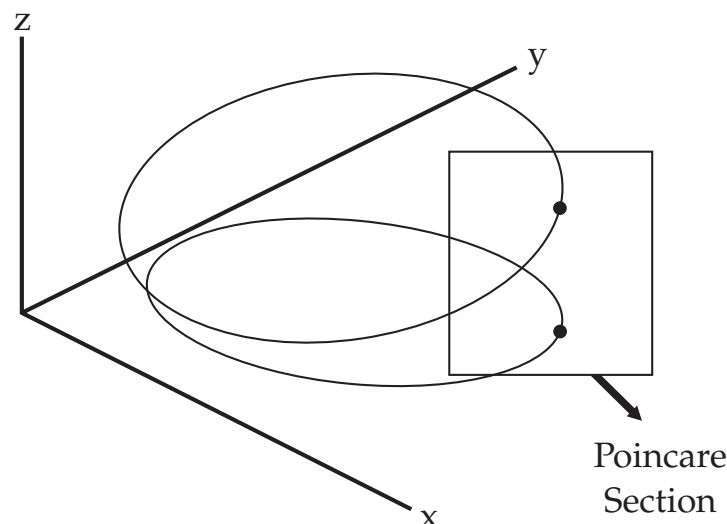


**Figure 8.** Graphical representation of calculating stroboscopic distribution by finding the points of intersection of the phase trajectories with the Poincare Section.

For visualization of the Poincare map for the proposed system, the plane  $x_2 = 0$  was taken as a Poincare section and the trajectories that crosses this section from  $x_2 < 0$  or  $x_2 > 0$  were recorded. Figure 7 shows the Poincare section for a different variation of the control parameter  $\beta$ . In Figure 7c, the trajectories cut the section in a single line (positive section of the grid), characterized by the quasi period-1 attractor given in Figure 7a. Similarly, the Poincare section for quasi period-2 and quasi period-4 are given in Figure 7f,i, characterized by the two or four straight lines in the Poincare section. Finally, in Figure 7l, the points are located irregularly on the Poincare section, the behavior of the system can be termed as chaotic as evident from the phase portrait given in Figure 7j.

## 6. Experimental Setup

To validate the numerical results of the proposed discrete map based jerk chaotic system, an electrical circuit was made. Op-Amps were used to implement the system of ODEs given by Equations (7), (8) and (10) [38]. Two analog multipliers ICs (AD633JR) were required in series to get the cubic term in Equation (10). It has four inputs ( $X_1, X_2, Y_1$  &  $Y_2$ ) and two outputs ( $W$  &  $Z$ ). The output is given as  $W = (X_1 - X_2) * (Y_1 - Y_2)/10 + Z$ . It

can be shown that the Equations (7), (8) and (10) [38] can be easily transformed into the following set of Equations (17)–(19).

$$\frac{dX_1}{dt} = \frac{X_2}{RC} \tag{17}$$

$$\frac{dX_2}{dt} = \frac{X_3}{RC} \tag{18}$$

$$\frac{dX_3}{dt} = \frac{X_1}{R_1C} - \frac{X_2}{R_2C} - \frac{X_3}{R_3C} - \frac{X_1^3}{600R_4C} \tag{19}$$

Using a time constant of  $1 \times 10^{-4}$ , the control parameters in terms of resistance and capacitor can be calculated from the following relations while maintaining the critical relation of  $R_4 = R/100$

$$\alpha = \frac{1 \times 10^{-4}}{R_1C} = 1, \quad \beta = \frac{1 \times 10^{-4}}{R_2C} = \text{Variable}, \tag{20}$$

$$\sigma = \frac{1 \times 10^{-4}}{R_3C} = 6, \quad \gamma = \frac{1 \times 10^{-4}}{600R_4C} = 6 \tag{21}$$

NI Multisim was used to simulate the electrical circuit before implementing it on the breadboard. The schematic of the proposed circuit is shown in Figure 9.

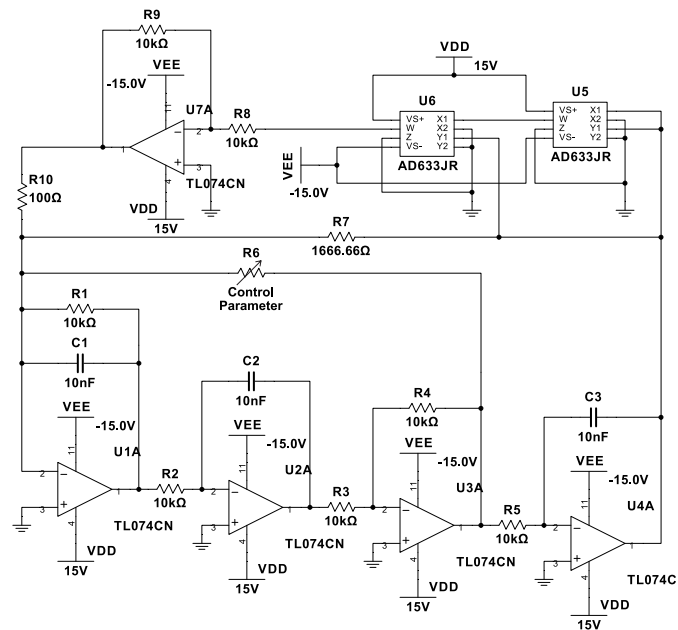


Figure 9. The circuit schematic for the proposed discrete-time map based jerk chaotic system.

Using appropriate time scaling, the output voltage of  $U_1A$  ( $x_3$ ) and  $U_3A$  ( $x_2$ ) are directly monitored using a two-channel digital oscilloscope shown in Figure 10.

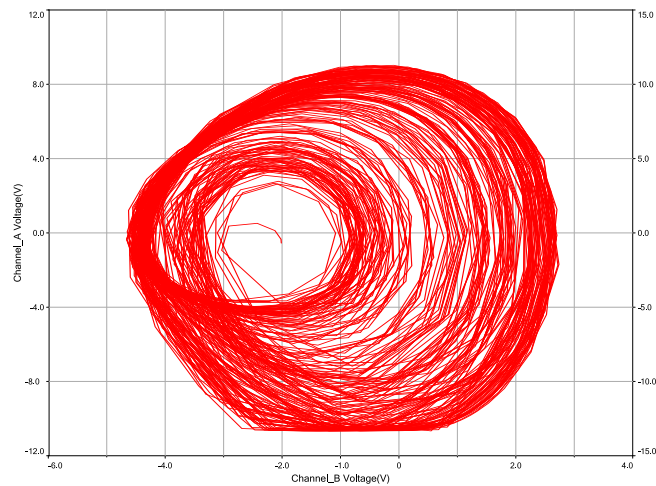


Figure 10. NI Multisim’s digital oscilloscope output for the proposed circuit with  $R_6 = 1807 \Omega$ .

*Experimental Verification*

The circuit schematic, given in Figure 9, was implemented on a breadboard by using TL074CN fast switching Op-Amps with high precision resistors, as shown in Figure 11. The values for the components of the circuit are tabulated in Table 1. Variable resistor ‘R6’ is used to replicate the effect of change of  $\beta$  in the numerical simulations. The proposed system shows period-doubling route to chaos as the value of R6 increases beyond 1 k $\Omega$ . Table 2 summarizes the various attractor obtained by changing the control resistance ‘R6’.

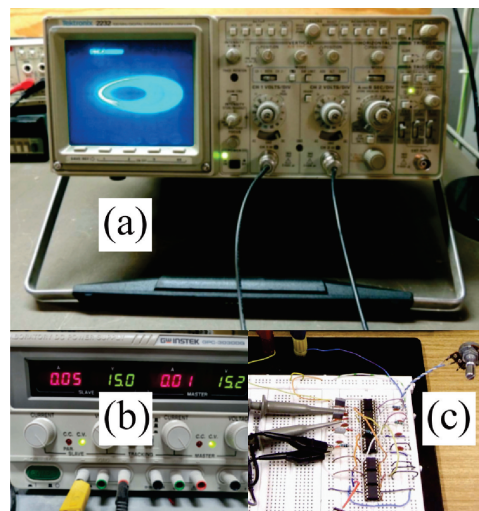


Figure 11. Experimental Setup: (a) Oscilloscope, (b) Controlled DC Power Supply, (c) Breadboard Implementation.

Table 1. Parameters of Experimental Setup.

Parameter	Value	Unit
R1–R5, R8–R9	10 k	$\Omega$
R7	1.67 k	$\Omega$
R10	100	$\Omega$
C1–C3	10 n	F
$V_{DD}$	15	V
$V_{EE}$	–15	V

**Table 2.** Summary of Different Attractor with the variation of Control Resistance R6.

Sr. No.	Value of R6	Attractor Type
1	1112 $\Omega$	Period 1
2	1667 $\Omega$	Period 2
3	1715 $\Omega$	Period 4
4	1807 $\Omega$	Chaotic Attractor

Figure 12 shows a comparison between the numerical (left) and hardware (right) results. Period 1 (limit cycle) attractor was obtained by setting the control resistor R6 to 1112  $\Omega$ , similarly increasing the value of R6 to 1667  $\Omega$  gives the period 2 attractor, R6 = 1715  $\Omega$  corresponds to period 4 attractor finally, R6 = 1807  $\Omega$  gives the chaotic attractor.

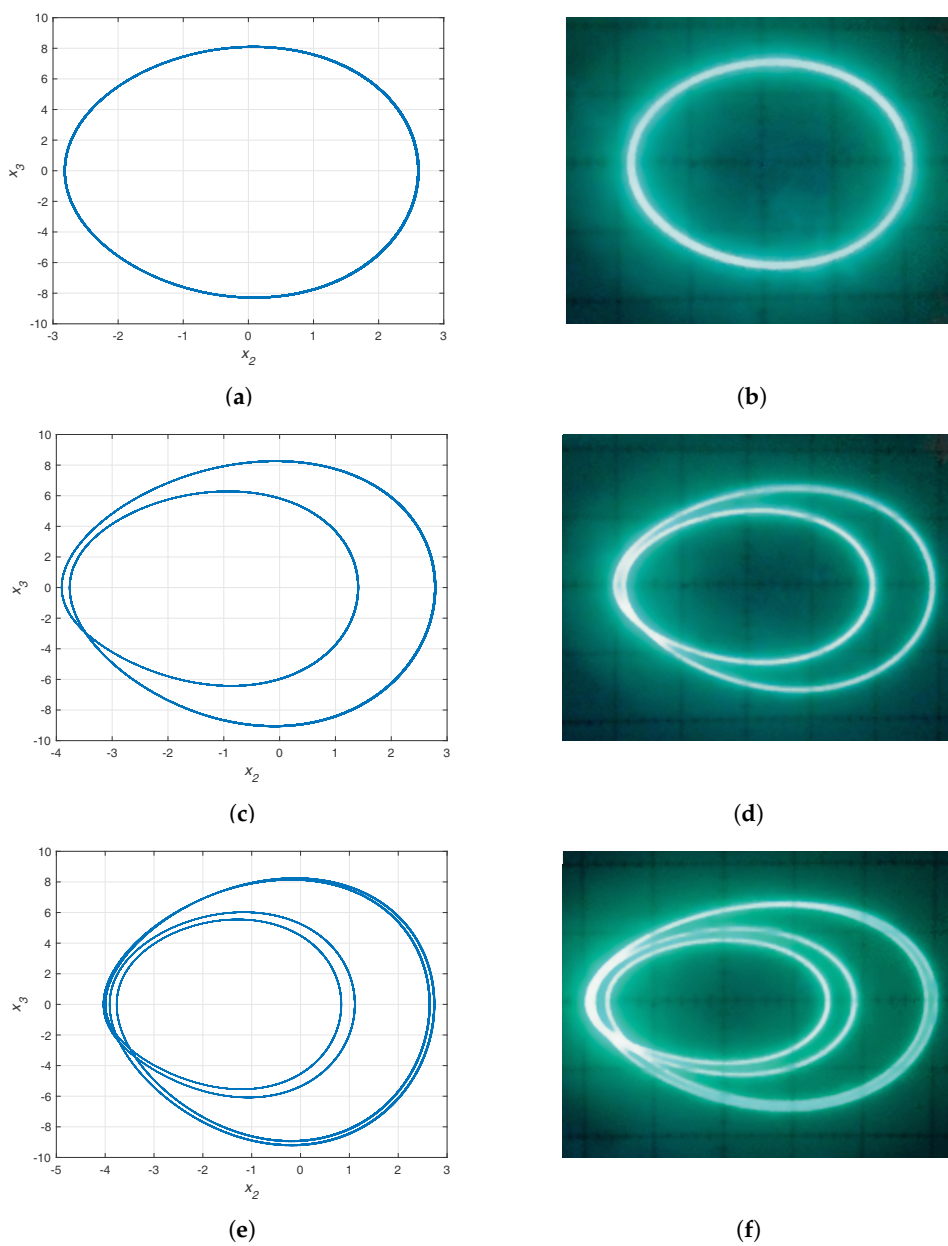


**Figure 12.** Cont.

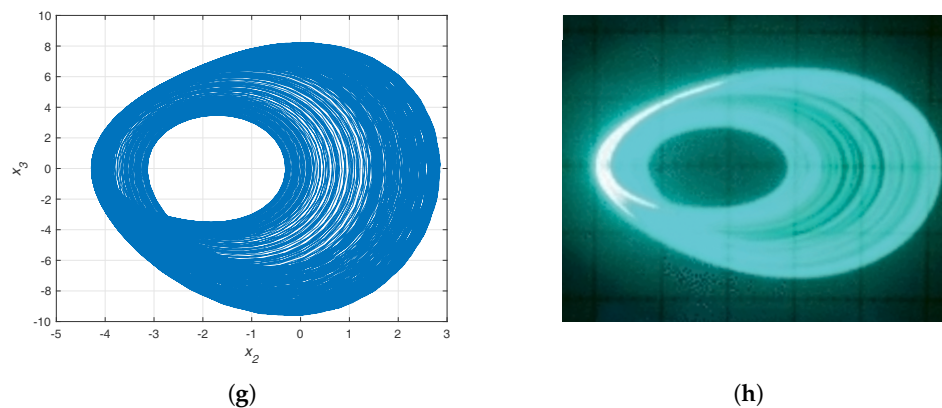


**Figure 12.** Numerical (left) vs. Experimental (right) results: (a,b) Period 1 or Limit Cycle Attractor case for  $\beta = 9$  &  $R_6 = 1112 \Omega$ , (c,d) Period 2 Attractor case for  $\beta = 6$  &  $R_6 = 1667 \Omega$ , (e,f) Period 4 Attractor case for  $\beta = 5.84$  &  $R_6 = 1715 \Omega$ , (g,h) Chaotic Attractor case for  $\beta = 5.535$  &  $R_6 = 1807 \Omega$ .

## 7. Discussion

Nonlinear dynamical systems with complex and irregular behavior can be characterized using chaotic time-series analysis. This method aims to study characteristics of the deterministic dynamical systems with different tools, describe them with a proper model, and predict future values. Since all practical systems are nonlinear, the analysis of a nonlinear dynamical system involves linearization. But, these hidden non-linearities produce strange behavior. Most of the engineering curriculum emphasizes the analysis of a system based on linear system theory [36], thereby oversimplifying the wide range of fascinating dynamic responses.

During the last century, many chaos theorists highlighted the educational importance of chaotic dynamical systems to pay off the conventional linear thinking established through prolonged learning techniques [43–45]. Nonlinear systems can exhibit complicated dynamics that disobey almost every law studied under linear systems. Because of several equilibrium points for different initial conditions, it becomes impossible to predict their long-term behavior. This property of the nonlinear system, which happens to be considered noise as it appears random in the time domain, can find its application in almost every scientific field. Overall, chaos theory enables us to embrace all the weirdness of life rather than suppressing it.

In this paper, a novel chaotic system is presented based on the simple jerk equation. The discrete sine map was added as a nonlinear function to the jerk equation and approximated using the Taylor series expansion. The proposed system simulation was carried out in MATLAB/NI Multisim first and later verified by hardware implemented using simple Op-Amps with analog multipliers.

## 8. Conclusions

This paper studied a simple nonlinear dynamical system based on a jerk equation with a discrete-time map. The system can show periodic as well as aperiodic behavior based on the value of the control parameter. MATLAB simulations were used to verify the theoretical aspects of the proposed system. An electronic circuit of the nonlinear system was made in NI Multisim using basic electrical engineering knowledge. Further, it was implemented in real-time on a breadboard to verify the system's chaotic nature. A fair consensus was seen between the simulation & experimental results. High frequency range, quasi-periodicity, autonomous chaotic existence, and low power consumption are some of the important aspects of the design, which can find applications in cryptography, secure communication, compressed sensing, biology, weather forecasting, mechanical engineering etc.

**Author Contributions:** Conceptualization, M.H.A. and M.K.; methodology, M.H.A.; software, M.H.A.; validation, M.H.A. and M.K.; formal analysis, M.H.A.; investigation, M.H.A., M.K. and M.A.A.; resources, A.E.H. and M.K.; writing—original draft preparation, M.H.A.; writing—review and editing, A.E.H., M.K. and M.A.A.; supervision, M.K.; project administration, M.K.; funding acquisition, A.E.H., M.K. and M.A.A. All authors have read and agreed to the published version of the manuscript.

**Funding:** The authors would like to acknowledge the support provided by King Fahd University of Petroleum & Minerals through the Research Group funded project #DF191004. The authors also acknowledge the funding support by King Abdullah City for Atomic and Renewable Energy (K.A. CARE), Energy Research & Innovation Center (ERIC) at KFUPM.

**Institutional Review Board Statement:** Not applicable.

**Informed Consent Statement:** Not applicable.

**Data Availability Statement:** The data presented in this study are available within the article.

**Acknowledgments:** The authors would like to acknowledge the support provided by King Fahd University of Petroleum & Minerals through the Research Group funded project #DF191004. The authors also acknowledge the funding support by King Abdullah City for Atomic and Renewable Energy (K.A. CARE), Energy Research & Innovation Center (ERIC) at KFUPM. We would like to acknowledge Anas Muhammad Rafiq for his assistance with the experimental verification.

**Conflicts of Interest:** The authors declare no conflict of interest.

## Abbreviations

The following abbreviations are used in this manuscript:

MLE	Maximum Lyapunov Exponent
ODE	Ordinary differential equation
SNFS	Saturated Nonlinear Function Series
DOF	Degree of freedom
H.O.T.	Higher-order terms
DSR	Deanship of Scientific Research
K. A. CARE	King Abdullah City of Atomic & Renewable Energy

## References

- Li, T.Y.; Yorke, J.A. Period Three Implies Chaos. *Am. Math. Mon.* **1975**, *82*, 985–992. [[CrossRef](#)]
- Oestreicher, C. A History of Chaos Theory. *Dialogues Clin. Neurosci.* **2007**, *9*, 279. [[PubMed](#)]
- Sundar, S.; Minai, A.A. Synchronization of Randomly Multiplexed Chaotic Systems with Application to Communication. *Phys. Rev. Lett.* **2000**, *85*, 5456. [[CrossRef](#)] [[PubMed](#)]
- Kotulski, Z.; Szczepański, J.; Górski, K.; Paszkiewicz, A.; Zugaj, A. Application of Discrete Chaotic Dynamical Systems in Cryptography - DCC Method. *Int. J. Bifurc. Chaos* **1999**, *9*, 1121–1135. [[CrossRef](#)]
- Krysko, A.; Awrejcewicz, J.; Zhigalov, M.; Pavlov, S.; Krysko, V. Nonlinear behaviour of different flexible size-dependent beams models based on the modified couple stress theory. Part 2. Chaotic dynamics of flexible beams. *Int. J. Non-Linear Mech.* **2017**, *93*, 106–121. [[CrossRef](#)]
- Awrejcewicz, J.; Krysko, A.; Kutepov, I.; Zagniboroda, N.; Dobriyan, V.; Krysko, V. Chaotic dynamics of flexible Euler-Bernoulli beams. *Chaos Interdiscip. J. Nonlinear Sci.* **2013**, *23*, 043130. [[CrossRef](#)]
- Arshad, M.H.; Kassas, M. A Chaos Based SVPWM technique for B4 Inverter fed Two-Phase Symmetric Induction Motor for THD & EMI improvement at Low Modulation Index. In Proceedings of the 2019 IEEE Texas Power and Energy Conference (TPEC), College Station, TX, USA, 7–8 February 2019; pp. 1–6.
- Ian, S. *Does God Play Dice?: The Mathematics of Chaos*; Blackwell Publishing: Hoboken, NJ, USA, 1989; p. 393.
- Sayed, W.S.; Radwan, A.G.; Fahmy, H.A. Chaotic Systems Based on Jerk Equation and Discrete Maps with Scaling Parameters. In Proceedings of the IEEE 2017 6th International Conference on Modern Circuits and Systems Technologies (MOCAST), Thessaloniki, Greece, 4–6 May 2017; pp. 1–4.
- Eckmann, J.P.; Ruelle, D. Ergodic Theory of Chaos and Strange Attractors. In *The Theory of Chaotic Attractors*; Springer: Berlin/Heidelberg, Germany, 1985; pp. 273–312.
- Sprott, J. Some Simple Chaotic Jerk Functions. *Am. J. Phys.* **1997**, *65*, 537–543. [[CrossRef](#)]
- Kennedy, M.P. Experimental Chaos from Autonomous Electronic Circuits. *Philos. Trans. R. Soc. Lond. Ser. A Phys. Eng. Sci.* **1995**, *353*, 13–32.

13. Lakshmanan, M.; Murali, K. Experimental Chaos from Non-Autonomous Electronic Circuits. *Philos. Trans. R. Soc. Lond. Ser. A Phys. Eng. Sci.* **1995**, *353*, 33–46.
14. Linsay, P.S. Period Doubling and Chaotic Behavior in a Driven Anharmonic Oscillator. *Phys. Rev. Lett.* **1981**, *47*, 1349. [[CrossRef](#)]
15. Newcomb, R.; Sathyan, S. An RC Op-Amp Chaos Generator. *IEEE Trans. Circuits Syst.* **1983**, *30*, 54–56. [[CrossRef](#)]
16. Matsumoto, T.; Chua, L.; Komuro, M. The Double Scroll Bifurcations. *Int. J. Circuit Theory Appl.* **1986**, *14*, 117–146. [[CrossRef](#)]
17. Azzouz, A.; Duhr, R.; Hasler, M. Transition to Chaos in a Simple Nonlinear Circuit Driven by a Sinusoidal Voltage Source. *IEEE Trans. Circuits Syst.* **1983**, *30*, 913–914. [[CrossRef](#)]
18. Kennedy, M.P. Chaos in the Colpitts Oscillator. *IEEE Trans. Circuits Syst. I Fundam. Theory Appl.* **1994**, *41*, 771–774. [[CrossRef](#)]
19. Tekam, R.B.W.; Kengne, J.; Kenmoe, G.D. High Frequency Colpitts' Oscillator: A Simple Configuration for Chaos Generation. *Chaos Solitons Fractals* **2019**, *126*, 351–360. [[CrossRef](#)]
20. Madan, R.N. *Chua's Circuit: A Paradigm for Chaos*; World Scientific Publishing Co.: Singapore, 1993.
21. Prebianca, F.; Marcondes, D.W.; Albuquerque, H.A.; Beims, M.W. Exploring an Experimental Analog Chua's Circuit. *Eur. Phys. J. B* **2019**, *92*, 134. [[CrossRef](#)]
22. Tchitnga, R.; Nguazon, T.; Fotso, P.H.L.; Gallas, J.A. Chaos in a Single Op-Amp-based Jerk Circuit: Experiments and Simulations. *IEEE Trans. Circuits Syst. II Express Briefs* **2015**, *63*, 239–243. [[CrossRef](#)]
23. Chiu, R.; López-Mancilla, D.; Castañeda, C.E.; Orozco-López, O.; Villafañá-Rauda, E.; Sevilla-Escoboza, R. Design and Implementation of a Jerk Circuit using a Hybrid Analog–Digital System. *Chaos Solitons Fractals* **2019**, *119*, 255–262. [[CrossRef](#)]
24. Radwan, A.; Soliman, A.M.; Elwakil, A.S. 1-D Digitally-Controlled Multiscroll Chaos Generator. *Int. J. Bifurc. Chaos* **2007**, *17*, 227–242. [[CrossRef](#)]
25. Bao, B.; Zhou, G.; Xu, J.; Liu, Z. Multiscroll Chaotic Attractors from a Modified Colpitts Oscillator Model. *Int. J. Bifurc. Chaos* **2010**, *20*, 2203–2211. [[CrossRef](#)]
26. Zidan, M.A.; Radwan, A.G.; Salama, K.N. Controllable V-shape multiscroll butterfly attractor: System and circuit implementation. *Int. J. Bifurc. Chaos* **2012**, *22*, 1250143. [[CrossRef](#)]
27. Sánchez-López, C.; Trejo-Guerra, R.; Muñoz-Pacheco, J.; Tlelo-Cuautle, E. N-Scroll Chaotic Attractors from Saturated Function Series Employing CCII+ s. *Nonlinear Dyn.* **2010**, *61*, 331–341. [[CrossRef](#)]
28. Sánchez López, C. A 1.7 MHz Chua's Circuit using VMs and CF+ s. *Rev. Mex. De Física* **2012**, *58*, 86–93.
29. Ortega-Torres, E.; Sánchez-López, C.; Mendoza-López, J. Frequency Behavior of Saturated Nonlinear Dunction Series Based on Opamps. *Rev. Mex. Física* **2013**, *59*, 504–510.
30. Sprott, J.C. A New Class of Chaotic Circuit. *Phys. Lett. A* **2000**, *266*, 19–23. [[CrossRef](#)]
31. Komuro, M. Birth and Death of the Double Scroll. In Proceedings of the 1985 24th IEEE Conference on Decision and Control, Fort Lauderdale, FL, USA, 11–13 December 1985; pp. 456–460.
32. Matsumoto, T.; Chua, L.; Komuro, M. Birth and Death of the Double Scroll. *Phys. D Nonlinear Phenom.* **1987**, *24*, 97–124. [[CrossRef](#)]
33. Patidar, V.; Sud, K. Bifurcation and Chaos in Simple Jerk Dynamical Systems. *Pramana* **2005**, *64*, 75–93. [[CrossRef](#)]
34. Kengne, J.; Njikam, S.; Signing, V.F. A Plethora of Coexisting Strange Attractors in a Simple Jerk System with Hyperbolic Tangent Nonlinearity. *Chaos Solitons Fractals* **2018**, *106*, 201–213. [[CrossRef](#)]
35. Kengne, J.; Mogue, R.L.T.; Fozin, T.F.; Telem, A.N.K. Effects of Symmetric and Asymmetric Nonlinearity on the Dynamics of a Novel Chaotic Jerk Circuit: Coexisting Multiple Attractors, Period Doubling Reversals, Crisis, and Offset Boosting. *Chaos Solitons Fractals* **2019**, *121*, 63–84. [[CrossRef](#)]
36. Tagne, R.M.; Kengne, J.; Negou, A.N. Multistability and chaotic dynamics of a simple Jerk system with a smoothly tuneable symmetry and nonlinearity. *Int. J. Dyn. Control* **2019**, *7*, 476–495. [[CrossRef](#)]
37. Giakoumis, A.; Volos, C.K.; Stouboulos, I.N.; Kyprianidis, I.M.; Nistazakis, H.E.; Tombras, G.S., Implementation of a Laboratory-based Educational Tool for Teaching Nonlinear Circuits and Chaos. In *Advances and Applications in Chaotic Systems*; Springer: Berlin/Heidelberg, Germany, 1995; pp. 379–407.
38. Chen, C.T. *Linear System Theory and Design*; Oxford University Press, Inc.: Oxford, UK, 1998.
39. Tancredi, G.; Sánchez, A.; Roig, F. A Comparison Between Methods to Compute Lyapunov Exponents. *Astron. J.* **2001**, *121*, 1171. [[CrossRef](#)]
40. Greiner, W. Lyapunov Exponents and Chaos. In *Classical Mechanics: Systems of Particles and Hamiltonian Dynamics*; Springer: Berlin/Heidelberg, Germany, 2010; pp. 503–516.
41. Sprott, J.C.; Sprott, J.C. *Chaos and Time-Series Analysis*; Oxford University Press, Inc.: Oxford, UK, 2003; Volume 69,
42. Awrejcewicz, J.; Krysko, A.; Soldatov, V.; Krysko, V. Analysis of the nonlinear dynamics of the Timoshenko flexible beams using wavelets. *J. Comput. Nonlinear Dyn.* **2012**, *7*, 011005. [[CrossRef](#)]
43. Seshadri, H.; Verma, K. The Embedding Theorems of Whitney and Nash. *Resonance* **2016**, *21*, 815–826. [[CrossRef](#)]
44. May, R.M. Simple Mathematical Models with very Complicated Dynamics. In *The Theory of Chaotic Attractors*; Springer: Berlin/Heidelberg, Germany, 2004; pp. 85–93.
45. Strogatz, S.H. *Nonlinear Dynamics and Chaos: With Applications to Physics, Biology, Chemistry, and Engineering*; CRC Press: Boca Raton, FL, USA, 2018.